Available online at www.sciencedirect.com

ScienceDirect

Procedia Structural Integrity 79 (2026) 233–238

Structural Integrity Procedia

www.elsevier.com/locate/procedia

28th International Conference on Fracture and Structural Integrity - 3rd Mediterranean Conference on Fracture and Structural Integrity

Fatigue crack growth in EB-PBF processed titanium alloys: impact of manufacturing parameters

C. Bellini[a]*, F. Berto[b], R. Borrelli[c], V. Di Cocco[a], S. Franchitti[c], P. Di Giamberardino[d], D. Iacoviello[d], S. Natali[b], D. Pilone[b], C. Schillaci[b]

[a]DICeM, University of Cassino and Southern Lazio, Via G. di Biasio 43,03043 Cassino, Italy
[b]DICMA, Sapienza University of Rome, Via Eudossiana 18, 00184 Rome, Italy
[c]Additive Manufacturing LAB, CIRA, Via Maiorise 1, 81043 Capua, Italy
[d]DIAG, Sapienza University of Rome, Via Ariosto 25, 00184 Rome, Italy

Abstract

Knowing and managing the fatigue performance of Ti6Al4V alloy when produced using Electron Beam – Powder Bed Fusion (EB-PBF) is essential due to its extensive use in demanding aerospace and medical applications. The main goal of this study is to systematically evaluate how beam current and scan speed affect the tensile strength and fatigue behaviour of Ti-6Al-4V produced by EB-PBF. To isolate their impacts, the machine was operated in manual mode with constant parameter settings, in contrast to standard EB-PBF operations.
The findings unequivocally showed that the different process parameters and the resulting microstructure and fatigue properties were directly correlated. Denser materials with lower porosity were produced by higher energy densities, which were attained by particular beam current and scan speed combinations. This greatly improved the specimens' mechanical characteristics and fatigue performance. These conclusions lay the basis for future optimisation, potentially leveraging artificial intelligence to estimate and attain desired material characteristics under stress while minimising manufacturing defects.

© 2025 The Authors. Published by ELSEVIER B.V.
This is an open access article under the CC BY-NC-ND license (https://creativecommons.org/licenses/by-nc-nd/4.0)
Peer-review under responsibility of IGF28 - MedFract3 organizers

Keywords: EB-PBF; Ti6Al4V; Fatigue propagation crack; Process parameters.

* Corresponding author. Tel.: +39 0776 299 3617.
E-mail address: costanzo.bellini@unicas.it

2452-3216 © 2025 The Authors. Published by ELSEVIER B.V.
This is an open access article under the CC BY-NC-ND license (https://creativecommons.org/licenses/by-nc-nd/4.0)
Peer-review under responsibility of IGF28 - MedFract3 organizers
10.1016/j.prostr.2025.12.329

1. Introduction

Additive Manufacturing (AM) has rapidly gained its position as a pivotal technique within advanced manufacturing. This manufacturing process allows engineers to produce parts directly from their digital model, regardless of how intricate their geometry might be, as stated by Frazier (2014) and Borrelli et al. (2024). Within the vast options of AM methods, the Powder Bed Fusion (PBF) family is truly important. These techniques, which rely on a high-energy source to strategically melt layers of fine metallic powders, are widely adopted for fabricating premium, fit-for-purpose components. The Electron Beam – Powder Bed Fusion (EB-PBF) process gained specific attention for this work. In fact, it has the unique capability to process reactive alloys at high temperatures in a vacuum environment. According to Murr et al. (2012) and Körner (2016), this characteristic yields parts that boast minimal contamination and substantially lower residual stresses than those produced via equivalent laser-based methods.

Without doubt, the Ti6Al4V alloy represents an important candidate for EB-PBF application. Thanks to its combination of superior specific strength, excellent resistance to corrosion, and intrinsic biocompatibility, it can be adopted in several demanding sectors: aerospace, defence, and biomedical implantation, as referred by Bellini et al. (2024b) and Cantaboni et al. (2024). The combination of design possibilities offered by EB-PBF and the robust characteristics of Ti6Al4V embodies a natural evolution towards producing advanced structural parts like patient-specific orthopaedic solutions and complex aeronautical components (Bellini et al. (2023), Epasto et al. (2019)). Fatigue life is frequently the single most influential design constraint in these fields, given the potential for truly catastrophic consequences should a structural failure occur.

The mechanical performance of parts fabricated via EB-PBF is inextricably linked to the specific thermal history the material undergoes during the layer-by-layer build-up. As Kobryn and Semiatin (2001) found, the process involves rapid, localised electron-beam heating followed by cooling into the already solidified substrate, yielding steep thermal gradients and rapid, non-equilibrium solidification kinetics. It is this dynamic process that ultimately governs the resulting material microstructure and dictates where and how process-induced flaws might appear. In Ti6Al4V, the EB-PBF cycle typically generates a distinctive structure dominated by columnar prior-β grains. These grains grow epitaxially, spanning across numerous layers, and are aligned primarily with the direction of heat extraction, that coincides with the build axis (Z-axis), as stated by Al-Bermani et al. (2010) and Tan et al. (2015). Subsequently, during the cooling phase, a finer α+β lamellar structure, often referred to as Widmanstätten or basket-weave, forms within these prior-β grains, as described by Gong et al. (2014) and Schillaci et al. (2025). This hierarchical, highly-textured microstructure is fundamentally unlike the more equiaxed grains found in traditionally cast or forged Ti6Al4V, a difference which consequently imposes a marked mechanical anisotropy, as asserted by Rafi et al. (2013) and Bellini et al. (2024a).

The process parameters influence the mechanical behaviour of EB-PBF processed alloys. Fleishel et al. (2023) produced samples of Ti6Al4V by changing the focus offset, a parameter controlling the energy concentration. In this manner, they were able to obtain defects like lack of fusion. They found an unexpected increase in the fatigue life due to the particular microstructure given by the lower focus offset. Similar research was carried out by Ran et al. (2020), who found that the speed factor affected the density and the yield strength of the processed titanium alloy. Silvestri et al. (2020) produced titanium specimens through EB-PBF by varying line offset, beam current, and scan speed while maintaining constant energy density. They discovered that, despite the energy density was the same, the attained properties varied, due to the interaction between the material electrons and those of the beam.

Therefore, the leading scope of this study is to methodically investigate the influence of the manufacturing parameters on the fatigue behaviour of Ti6Al4V specimens manufactured via EB-PBF. To detect this effect, plates were fabricated by varying the beam current and the beam speed. From these plates, Compact Tension (CT) specimens were machined to evaluate fatigue properties. The study was completed by a detailed scanning electron microscopy (SEM) analysis of the fracture surfaces to identify crack initiation and propagation mechanisms and correlate them with the observed fatigue performance.

2. Materials and methods

As far as the specimen is concerned, the Compact Tension type was chosen, according to the ASTM E647 standard. It presented a thickness of 8 mm and an almost square profile with a height of 50 mm and a width of 48 mm. The notch was 2,5 mm wide and its tip was located at 8 mm from the line between the centres of the holes for the loading pins. The titanium powder used in the present research activity was made of the Ti6Al4V alloy, a material commonly used in the aeronautical industry. The powder was provided by the manufacturer of the printing machine, so it had high quality. The particles showed a high sphericity, which is very important for this kind of process since this characteristic improves the flowability.

Concerning the process parameters, four different sets were generated by changing the beam current and the beam speed, as reported in Table 1. The other parameters, that are the hatch distance, the focus offset, the layer thickness, and the beam voltage were kept at a constant value. In this manner, different values of energy densities were obtained. In particular, the first set, the A, provided the highest energy, and this was necessary to obtain fully dense parts, without defects, while for the other sets the energy was lower, introducing different quantities of defects. Indeed, even if the parameters of the B and C sets were quite different, for instance, the C beam current was twice that of B, but the energy densities were quite similar because the beam speed compensated for the current difference.

Table 1. Manufacturing process parameters.

Set	s (mm/s)	I (mA)	h (mm)	FO (mA)	t (mm)	v (kV)	VED (J/mm3)
A	4530	15					39,74
B	6000	8	0,1	3	0,05	60	16,00
C	10000	15					18,00
D	9600	8					10,00

Specimens were manufactured by electron-beam powder bed fusion (PBF-EB) using an Arcam A2X system.. The printing steps are the typical ones of the EB-PBF process: after creating the geometry of the specimens, they were arranged in the working space and sliced through the Arcam Build Processor software. Subsequently, the machine was prepared for the manufacturing run: the powder hoppers were filled and the process parameters were set. Then, the vacuum was drawn in the manufacturing chamber, the electron beam was calibrated, and the manufacturing chamber was preheated. As the imposed temperature was reached, the specimens were built according to the typical sequence of a powder bed additive manufacturing process. At the end of the process, the chamber was cooled down and the specimens were extracted from the unmelted powder and cleaned. Finally, the holes for loading pins and the notch were added to the specimen through machining. One of the produced specimens is presented in Fig. 1.

Fig. 1. CT specimen for fatigue crack propagation test.

Fatigue crack growth tests were performed using a computer-controlled servohydraulic testing machine. For the experimental tests, a load ratio of 0.1 was employed. The other experimental conditions were a loading frequency of 30 Hz, a sinusoidal waveform and room temperature environment. To accurately evaluate the crack length, a compliance method was implemented. This technique uses the relationship between the specimen deformation and the length of the crack. The procedure involved using a double cantilever mouth gage to precisely measure the crack opening displacement (COD), that was correlated to the actual crack length using established calibration equations. For validation, the crack length measurements from the compliance method were checked using a standard optical method.

3. Results

In this paragraph, Paris' curves for the tested material are described. The graph, reported in Fig. 2, plots the fatigue crack growth rate da/dN as a function of the stress intensity factor range ΔK on a log-log scale. The specimen D, in green, was the worst performer, with its curve positioned to the left and above the others, while the specimens A, B, and C, represented in blue, red, and yellow, respectively, performed significantly better than D. In fact, their curves were shifted noticeably to the right, indicating superior resistance to crack growth. The specimen A appeared to offer the best performance, even if the difference with B and C was not so high. It must be remembered that, in the standard Paris plot, a curve positioned lower and to the right indicates superior material performance, since a higher driving force ΔK is needed for the crack to grow at the same rate.

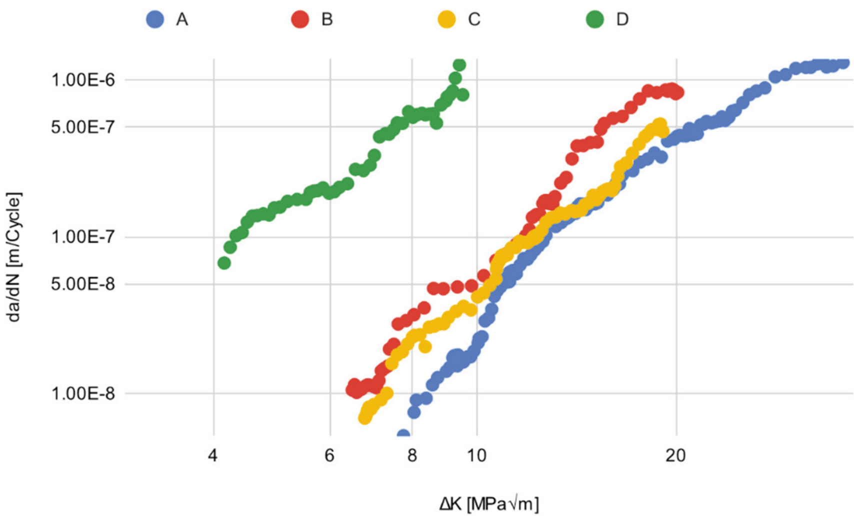

Fig. 2. Fatigue crack propagation curves for the tested specimens.

To better explain the fatigue crack growth behaviour, SEM images of the fracture surfaces of the broken specimens were obtained and are presented in Fig. 3. The micrographs relevant to the A and B specimens displayed relatively uniform and flat fracture surfaces, that are characteristic of a trans-granular fracture mode. The absence of significant defects like pores or unmelted powder indicates that process parameters used for fabricating A and B specimens, achieved high material density and effective metallurgical bonding. This type of surface is expected from a high-quality additively manufactured part undergoing stable fatigue crack growth. The surface of the C specimen appears rougher and more topographically complex than A and B. Moreover, a lack of fusion defect can be observed on the left of the image, as denoted by the very smooth surface of that zone. The fracture surface of the D specimen is dominated by large, spherical and semi-sintered particles, and large smooth areas. These are unambiguous indicators of lack-of-fusion (LoF) porosity. LoF defects occur when the energy input during the EB-PBF process is insufficient to fully melt the metal powder particles, leaving voids in the final part. The LoFs are widely regarded as the most detrimental type of defect for fatigue life. Due to their size and often sharp geometry, they act as dangerous stress concentrators, effectively behaving as large pre-existing cracks. This allows for very rapid crack propagation, since the fracture has not propagated through a continuous material but has primarily followed this network of pre-existing voids, which requires significantly less energy.

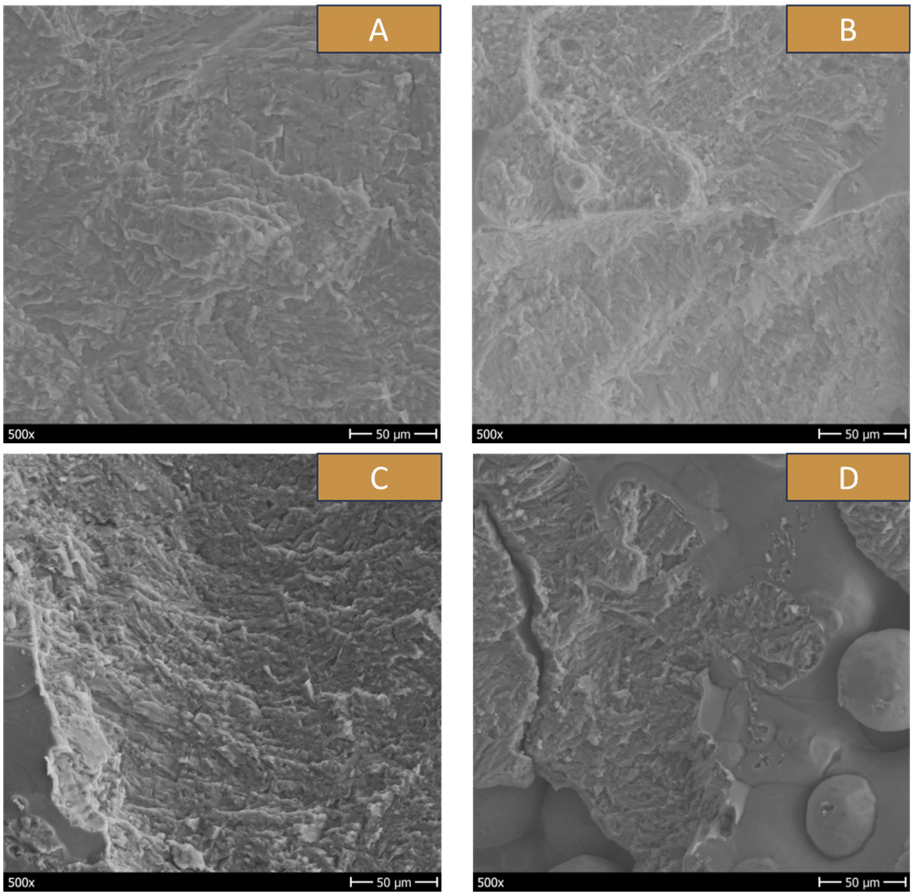

Fig. 3. Fracture surface of the tested specimens.

4. Conclusions

This study systematically investigated the influence of Electron Beam – Powder Bed Fusion (EB-PBF) process parameters on the fatigue crack growth (FCG) behaviour of Ti6Al4V. In particular, beam current and beam speed were investigated. The Paris curves generated from the Compact Tension (CT) specimens provided a clear demarcation of material performance, allowing for direct correlation between manufacturing inputs and final mechanical response.

The FCG analysis revealed a significant dependence on the selected parameters. Specimen D performed worst in fatigue crack growth: its Paris curve is displaced upward and leftward, consistent with reduced resistance to propagation. Conversely, specimens A, B, and C demonstrated superior fatigue performance, requiring a substantially higher stress intensity factor range to achieve the same crack growth rate.

Detailed Scanning Electron Microscopy (SEM) analysis of the fracture surfaces provided the critical evidence needed to explain these performance disparities. The fracture surfaces of the high-performing specimens, A and B, were characteristically uniform and flat, consistent with a stable, trans-granular fracture mode in a high-density material. The absence of significant defects confirmed that parameters A and B ensured effective metallurgical bonding and high material quality. On the contrary, the fracture surface of the worst-performing specimen (D) was dominated by large, spherical semi-sintered particles and extensive smooth areas, hallmarks of Lack-of-Fusion (LoF) porosity. The LoFs defects were the cause of the poor fatigue behaviour of specimen D.

Acknowledgements

This research was made possible with funding from the European Union – Next Generation EU, Mission 4 Component 1, which was administered through the Italian Ministry of University and Research as part of the PRIN 2022 program. The unique project code (CUP) for this work is H53D23001200006.

References

Al-Bermani, S. S., Blackmore, M. L., Zhang, W., Todd, I., 2010. The Origin of Microstructural Diversity, Texture, and Mechanical Properties in Electron Beam Melted Ti-6Al-4V. Metallurgical and Materials Transactions A 41 (13), 3422–3434.

Bellini, C., Borrelli, R., Di Caprio, F., Di Cocco, V., Franchitti, S., Iacoviello, F., Pirozzi, C., Sorrentino, L., 2023. Geometrical Accuracy Analysis of Ti-6Al-4V Trusses Manufactured by Electron Beam Melting Process. Metals 13 (8), 13081454.

Bellini, C., Borrelli, R., Di Cocco, V., Franchitti, S., Iacoviello, F., Mocanu, L. P., Sorrentino, L., 2024a. Effects of the Manufacturing Process on the Flexural Properties of EBMed Lattice Structures. Fatigue and Fracture of Engineering Materials and Structures 47 (12), 4729–4740.

Bellini, C., Borrelli, R., Di Cocco, V., Franchitti, S., Iacoviello, F., Mocanu, L. P., Sorrentino, L., 2024b. Titanium/FRP Hybrid Sandwich: In-Plane Flexural Behaviour of Short Beam Specimens. Frattura Ed Integrità Strutturale 18 (69), 18–28.

Borrelli, R., Bellini, C., Berto, F., Di Cocco, V., Foti, P., Iacoviello, F., Mocanu, L. P., Pirozzi, C., Razavi, N., 2024. The Impact of Ti6Al4V Powder Reuse on the Quality of Electron Beam Powder Bed Fusion Parts. Progress in Additive Manufacturing 9, 1475–1490.

Cantaboni, F., Battini, D., Hauber, K. Z., Ginestra, P. S., Tocci, M., Avanzini, A., Ceretti, E., Pola, A., 2024. Mechanical and Microstructural Characterisation of Ti6Al4V Lattice Structures with and without Solid Shell Manufactured via Electron Beam Powder Bed Fusion. The International Journal of Advanced Manufacturing Technology 131, 1289–1301.

Epasto, G., Palomba, G., D'Andrea, D., Guglielmino, E., Di Bella, S., Traina, F., 2019. Ti-6Al-4V ELI Microlattice Structures Manufactured by Electron Beam Melting: Effect of Unit Cell Dimensions and Morphology on Mechanical Behaviour. Materials Science and Engineering A 753 (November 2018), 31–41.

Fleishel, R., Ferrell, W., TerMaath, S., 2023. Fatigue-Damage Initiation at Process Introduced Internal Defects in Electron-Beam-Melted Ti-6Al-4V. Metals 13 (2), 13020350.

Frazier, W. E., 2014. Metal Additive Manufacturing: A Review. Journal of Materials Engineering and Performance 23 (6), 1917–1928.

Gong, X., Anderson, T., Chou, K., 2014. Review on powder-based electron beam additive manufacturing technology. Manufacturing Review 1, 2.

Kobryn, P. A., Semiatin, S. L., 2001. The Laser Additive Manufacture of Ti-6Al-4V. JOM 53 (9): 40–42.

Körner, C., 2016. Additive Manufacturing of Metallic Components by Selective Electron Beam Melting - A Review. International Materials Reviews 61 (5), 361–377.

Murr, L. E., Gaytan, S. M., Ramirez, D. A., Martinez, E., Hernandez, J., Amato, K. N., Shindo, P. W., Medina, F. R., Wicker, R. B., 2012. Metal Fabrication by Additive Manufacturing Using Laser and Electron Beam Melting Technologies. Journal of Materials Science and Technology 28 (1), 1–14.

Rafi, H. K., Karthik, N. V., Gong, H., Starr, T. L., Stucker, B. E., 2013. Microstructures and Mechanical Properties of Ti6Al4V Parts Fabricated by Selective Laser Melting and Electron Beam Melting. Journal of Materials Engineering and Performance 22 (12), 3872–3883.

Ran, J., Jiang, F., Sun, X., Chen, Z., Tian, C., Zhao, H., 2020. Microstructure and mechanical properties of ti-6al-4v fabricated by electron beam melting. Crystals 10(11), 0972.

Schillaci, C., Pilone, D., Berto, F., Bellini, C., Di Cocco, V., Di Giamberardino, P., Iacoviello, D., 2025. Correlation between process parameters and mechanical properties of Ti6Al4V alloys processed by electron beam melting. Fracture and Structural Integrity 74, 310–320.

Silvestri, A. T., Foglia, S., Borrelli, R., Franchitti, S.,Pirozzi, C., Astarita, A., 2020. Electron beam melting of Ti6Al4V: Role of the process parameters under the same energy density. Journal of Manufacturing Processes 60, 162–179.

Tan, X., Kok, Y., Tan, Y. J., Descoins, M., Mangelinck, D., Tor, S. B., Leong, K. F., Chua, C. K., 2015. Graded Microstructure and Mechanical Properties of Additive Manufactured Ti-6Al-4V via Electron Beam Melting. Acta Materialia 97, 1–16.